

# Theory of the coherent population trapping maser: A strong-field self-consistent approach

Aldo Godone,<sup>1</sup> Filippo Levi,<sup>1</sup> Salvatore Micalizio,<sup>2</sup> and Jacques Vanier<sup>3</sup>

<sup>1</sup>*Istituto Elettrotecnico Nazionale, Galileo Ferraris, Torino, Italy*

<sup>2</sup>*Politecnico di Torino, Torino, Italy*

<sup>3</sup>*Université de Montréal, Montréal, Canada*

(Received 24 July 2000; published 12 October 2000)

The phenomenon of coherent microwave stimulated emission in a cavity is analyzed for the case of alkali atoms such as Cs and Rb under coherent population trapping (CPT) in a  $\Lambda$  scheme. The calculations are made in transient and in continuous operation within the framework of a three level model. The coupling of the atoms to the microwave field generated inside the cavity by the atomic ensemble, is fully taken into account; it introduces radiation damping and an imbalance in the populations of the ground-state hyperfine levels, decreasing the intrinsic symmetry of the  $\Lambda$  scheme. The effect leads also to a broadening and to a frequency shift of the microwave emission profile. A comparison is made with the optically pumped alkali atom maser, allowing a deeper understanding of the CPT stimulated emission phenomenon.

PACS number(s): 32.80.Wr, 06.30.Ft, 31.15.Ne, 42.50.Md

## I. INTRODUCTION

The emission of coherent microwave radiation in a cavity at the hyperfine frequency of the ground state of alkali-metal atoms has been demonstrated for an atomic ensemble submitted to coherent population trapping (CPT) [1–3]. It was also shown that the microwave radiation is produced by the oscillating magnetization created in the atomic ensemble by the strong coherence generated by the  $\Lambda$  scheme excitation [4]. The phenomenon, as its name indicates, also has the property of trapping all atoms in the ground state. This trapping is responsible for the creation of a dark state in the ensemble, causing a dark line in the fluorescence spectrum [5]. Beside the fundamental physics interest of the CPT phenomenon, applications have been proposed in many fields such as atom cooling [6], lasing without inversion [7], magnetometry [8], and atomic frequency standards [9–11].

The characteristics of the microwave emission have been examined both theoretically and experimentally in Ref. [4], in view of the possible realization of a new atomic frequency standard: the ‘‘CPT maser’’ [3]. The theoretical analysis was done in the limit of low feedback (low cavity  $Q$  and/or low number of atoms) causing a negligible reaction of the microwave field on the atomic ensemble itself. However, the analysis showed that the coherent microwave emission could be interpreted as a stimulated emission process similar to that observed in hydrogen and rubidium masers [12,13].

In the present paper we develop a self-consistent theory of the CPT maser when the effect of the microwave field on the state of the atomic ensemble is not negligible relative to other relaxation and pumping mechanisms. The analysis is done in a self-consistent approach in which the effect of the field, amplitude and phase, calculated from the field equation, is introduced directly in the density-matrix rate equations. Several conclusions are drawn in connection to the presence of radiation damping, light shifts, power shifts, and cavity pulling. The calculation is extended also to the case of the intensity optically pumped maser (IOP maser) [14,15]. The analysis provides a natural transition from the CPT to the IOP maser. It is shown that the two types of masers,

although rather different relative to physical characteristics, are natural extensions of each other when the laser optical pumping scheme evolves from CPT to IOP or vice versa.

## II. RATE EQUATIONS AND POWER OUTPUT

The analysis is done for the general energy-level scheme shown in Fig. 1, representing two ground states  $\mu$  and  $\mu'$  and an excited  $m$  of an atomic ensemble connected by two coherent laser radiation fields. In particular our interest is focused on the case of an optically thin alkali atomic vapor (Cs, Rb, and Na) contained in a cell with buffer gas. The conceptual physical arrangement used in the analysis is shown in Fig. 2. Collisions of the alkali atoms with the buffer gas atoms cause homogeneous broadening of the excited  $P_{1/2}$  and  $P_{3/2}$  states. The excited-state decay rate  $\Gamma^*$  takes into account spontaneous emission and those colli-

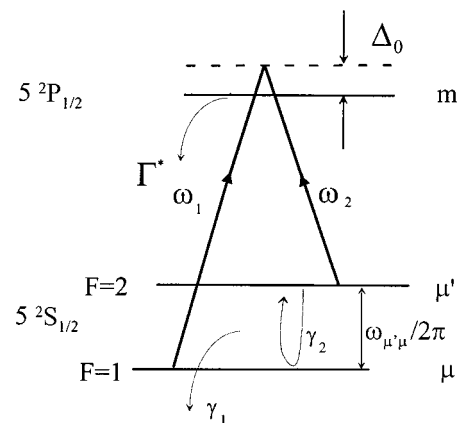


FIG. 1. Three-level system considered in the analysis (the  $D_1$  transition of  $^{87}\text{Rb}$  is reported as an example).  $\omega_1$  and  $\omega_2$  are the laser angular frequencies and  $\omega_{\mu',\mu}/2\pi$  is the hyperfine frequency shifted by various static perturbations described in the text.  $\Gamma^*$  is the decay rate from the excited state to the ground-state levels,  $\gamma_1$  and  $\gamma_2$  are the ground-state relaxation rates of the population difference and of the coherence, respectively, and  $\Delta_0$  is the lasers detuning from the optical resonance.

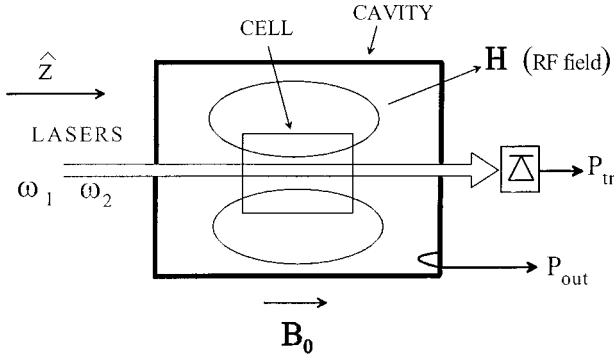


FIG. 2. Conceptual arrangement used in the theoretical analysis. The cavity operates in the mode  $TE_{011}$  resonates at the hyperfine frequency of the alkali-metal atom chosen.  $P_{out}$  is the microwave output power.

sions. When nitrogen is used as buffer gas, the decay takes place without fluorescence. This so-called quenching effect prevents a loss of coherence, which would be caused by the fluorescence radiation creating random optical pumping. At the buffer gas pressures considered in this paper, the resulting optical broadening is of the order of the excited-state hyperfine splitting. In practice, pumping is done by means of one of the two  $P$  states ( $D_1$  or  $D_2$  radiation). This state is approximated by the single level  $m$  shown in Fig. 1. The buffer gas is also used to reduce the ground-state hyperfine resonance broadening due to the transit time of the atoms across the laser beams and to inhibit Doppler broadening at the microwave frequency by means of the Dicke effect [16]. The rates  $\gamma_1$  and  $\gamma_2$  are, respectively, the population and coherence relaxation rates of the alkali atoms in the ground state, taking into account perturbations such as spin-exchange collisions, buffer gas collisions, and collisions of the atoms with the cell walls.

As shown in Fig. 2, a static magnetic induction  $\mathbf{B}_0$  is applied to the system and provides a quantization axis. This magnetic field splits the ground-state Zeeman levels and decouples them to the extent that they can be considered isolated. The two hyperfine levels in the ground state are those represented in Fig. 1 as  $\mu$  and  $\mu'$ , respectively. Static displacements of the energy levels due to the buffer gas collisions and the applied magnetic field are included in the definition of the various resonance frequencies. The cell containing the alkali atoms and the buffer gas is placed inside a microwave cavity operating in the  $TE_{011}$  mode. The cell is sufficiently small as to allow approximations in connection to the homogeneity of the microwave field over its volume. The transitions from the two ground-state hyperfine

levels to the  $P$  state are excited by means of coherent radiation fields that can be obtained in practice from either two phase-locked lasers or two sidebands of a single laser modulated at a subharmonic of the hyperfine frequency [10]. A  $\lambda/4$  plate shown produces circular polarization of the incoming laser beam, required by the selection rules encountered in the excitation process of the CPT phenomenon [17].

### A. Rate equations

The analysis is done as in Ref. [4] in the density-matrix formalism starting with the master equation describing the atomic ensemble (Liouville equation). The laser excitation is represented by the Rabi frequencies  $\omega_{R1}$  and  $\omega_{R2}$  defined as

$$\omega_{R1} = -(E_{01}/\hbar)\langle\mu|e\mathbf{r}\cdot\mathbf{e}_\lambda|m\rangle, \quad (1)$$

$$\omega_{R2} = -(E_{02}/\hbar)\langle\mu'|e\mathbf{r}\cdot\mathbf{e}_\lambda|m\rangle, \quad (2)$$

where  $E_{0i}$  is the laser field amplitude exciting transitions from either levels  $\mu$  or  $\mu'$ , and the terms within brackets are the dipole matrix elements of the transitions with  $\mathbf{e}_\lambda$  being the polarization vector. A microwave field is present in the cavity and is assumed to have the form

$$\mathbf{B}_{\mu w}(r,t) = \hat{\mathbf{z}}B_z(r)\cos(\omega_{12}t + \phi), \quad (3)$$

where  $B_z(r)$  is the microwave field amplitude,  $\omega_{12}$  is the frequency difference between the two laser fields ( $\omega_1 - \omega_2$ ), and  $\phi$  is the phase of this field, whose meaning will be made clear in the analysis. The Rabi frequency associated with this field is defined as

$$b(r) = -\mu_z\mu_0 H_z(r)/\hbar, \quad (4)$$

where  $\mu_z$  is the atom's magnetic moment and  $H_z$  is  $B_z/\mu_0$ ,  $\mu_0$  being the permeability of free space. In the case of alkali atoms for the  $m=0, \Delta m=0$  transition  $\mu_z = \mu_B$ , the Bohr magneton. We make the long wavelength and the rotating wave approximations and assume for the off-diagonal elements of the density matrix, solutions of the form

$$\begin{aligned} \rho_{\mu\mu'} &= \delta_{\mu\mu'} e^{i(\omega_1 - \omega_2)t}, \\ \rho_{\mu m} &= \delta_{\mu m} e^{i\omega_1 t}, \\ \rho_{\mu' m} &= \delta_{\mu' m} e^{i\omega_2 t}. \end{aligned} \quad (5)$$

It is assumed that the laser interaction is relatively weak and that at all times the population of the excited  $P$  state is small in comparison to that of the ground state. We obtain the following set of rate equations describing the response of the atomic ensemble to the applied fields:

$$\rho_{\mu\mu} + \rho_{\mu'\mu'} \approx 1, \quad (6)$$

$$\dot{\rho}_{mm} + \Gamma^* \rho_{mm} = \omega_{R1} \text{Im} \delta_{\mu m} + \omega_{R2} \text{Im} \delta_{\mu' m}, \quad (7)$$

$$\dot{\Delta} + \gamma_1 \Delta = 2b \text{Im}(e^{-i\phi} \delta_{\mu\mu'}) - \omega_{R2} \text{Im} \delta_{\mu' m} + \omega_{R1} \text{Im} \delta_{\mu m}, \quad (8)$$

$$\dot{\delta}_{\mu\mu'} + (\gamma_2 + i\Omega_\mu) \delta_{\mu\mu'} = -i \frac{b}{2} e^{i\phi} \Delta - i \frac{\omega_{R1}}{2} \delta_{m\mu'} + i \frac{\omega_{R2}}{2} \delta_{\mu m}, \quad (9)$$

$$\dot{\delta}_{\mu m} + \left( \frac{1}{2} \Gamma^* + i\Delta_0 \right) \delta_{\mu m} = i \frac{\omega_{R1}}{4} (1 - \Delta) + i \frac{\omega_{R2}}{2} \delta_{\mu\mu'}, \quad (10)$$

$$\dot{\delta}_{\mu'm} + \left( \frac{1}{2} \Gamma^* + i\Delta_0 \right) \delta_{\mu'm} = i \frac{\omega_{R2}}{4} (1 + \Delta) + i \frac{\omega_{R1}}{2} \delta_{\mu'\mu}. \quad (11)$$

The  $\rho_{ii}$  are the fractional populations of the various levels,  $\Delta = \rho_{\mu'\mu'} - \rho_{\mu\mu}$ , and the  $\delta_{ij}$  are the coherences in the interaction representation. We have defined

$$\Omega_\mu = (\omega_1 - \omega_2) - \omega_{\mu'\mu} \quad (12)$$

and  $\Delta_0$  the detuning between the lasers and the excited state (see Fig. 1). Equations (6)–(11) have been obtained introducing the following approximations widely satisfied in the usual experimental conditions:

$$\Omega_\mu \ll \Gamma^*, \quad b \ll \Gamma^*, \quad \omega_{R1,2} \ll \Gamma^*. \quad (13)$$

The system of rate equations (6)–(11) has been analyzed in Ref. [18] in the case  $b=0$ , leading to the explanation of the dark line observed in the fluorescence spectrum. The system has also been analyzed in Ref. [4], by means of a perturbation approach in which the oscillating magnetic field, although giving rise to stimulated emission of radiation, is small enough as not to affect the atomic ensemble population and coherence. In the present paper we will solve the above system of equations in a self-consistent approach in which the microwave field is not negligible and causes important effects on the behavior of the atomic ensemble.

## B. Field equation

### 1. Determination of the phase of the microwave field

The oscillating magnetic field in the cavity and the oscillating magnetization  $M(r, t)$  created in the ensemble by the CPT phenomenon [4], are coupled through the equation:

$$\mathbf{H}(\mathbf{r}) = \frac{-iQ_L}{1 + i2Q_L(\Delta\omega_c/\omega_{12})} \mathbf{H}_c(\mathbf{r}) \int_{V_c} \mathbf{H}_c(\mathbf{r}) \cdot \mathbf{M}(\mathbf{r}) dV, \quad (14)$$

where  $\mathbf{H}_c$  is the cavity field orthonormal mode,  $V_c$  is the cavity volume,  $Q_L$  is the loaded cavity quality factor, and  $\Delta\omega_c$  is the cavity detuning from  $\omega_{12}$ .  $M(r)$  acts as the source term and its value is obtained from the relation

$$\langle M(r, t) \rangle = \text{Tr}(M_{\text{op}} \rho), \quad (15)$$

where  $M_{\text{op}}$  is the quantum-mechanical operator representing the total magnetic moment and the symbol  $\langle \rangle$  means an average over the ensemble represented by  $\rho$ . Using the rotating wave approximation and keeping only the resonant term,  $M(r, t)$  is calculated as

$$M(r, t) dV = -(1/2) n \mu_B \delta_{\mu'\mu} e^{-i\omega_{12}t} dV, \quad (16)$$

where  $dV$  is a volume element and  $n$  is the atomic density. On the other hand, the resonant component of the field, according to Eq. (3), may be written as

$$H(r) = |H(r)| e^{-i\phi}. \quad (17)$$

We write explicitly the hyperfine coherence as  $\delta_{\mu\mu'} = \delta_{\mu\mu'}^r + i\delta_{\mu\mu'}^i$ , and by simple algebraic manipulations of the above equations we obtain

$$\phi = + \frac{\pi}{2} + \tan^{-1} 2Q_L \frac{\Delta\omega_c}{\omega_{12}} + \tan^{-1} \frac{\delta_{\mu\mu'}^i}{\delta_{\mu\mu'}^r}. \quad (18)$$

This expression sets the phase of the field in the rate equations (6)–(11). It is noted that in [4], the phase was set equal to  $\pi/2$ , and that the other terms were not considered in the analysis since the effect of the field on the atomic ensemble population and coherence was neglected.

### 2. The field amplitude and the Rabi frequency

The energy dissipated in the cavity near resonance ( $\Delta\omega_c \ll \omega_{\mu'\mu}/2Q_L$ ) is given by [19]

$$P_{\text{diss}} = \frac{\omega_{\mu'\mu} \mu_0}{2Q_L} \int_{V_c} |\mathbf{H}(\mathbf{r})|^2 dV. \quad (19)$$

On the other hand, following the computations reported in Ref. [4], the power given by the atoms is

$$P_{\text{diss}} = \frac{(1/2) \hbar \omega_{\mu'\mu} k N |2\delta_{\mu\mu'}|^2}{1 + 4Q_L^2 (\Delta\omega_c/\omega_{\mu'\mu})^2}, \quad (20)$$

where  $k$  is the so-called gain factor or the number of microwave photons emitted by an atom in 1 s. It is defined as

$$k = \frac{\mu_0 \mu_z^2 \eta' Q_L N}{\hbar V_a}, \quad (21)$$

where  $V_a$  is the effective volume of the cell containing the alkali atoms that are exposed to the radiation fields,  $N$  is the total number of atoms equal to  $nV_a$  and  $\eta'$  is the filling factor given by

$$\eta' = \frac{V_a \langle H_{cz}(r) \rangle_a^2}{V_c \langle H_c^2(r) \rangle_c}. \quad (22)$$

The symbols  $\langle \rangle_i$  represent a space average over the volume in question. The Rabi frequency is evaluated in a self-consistent approach in which the energy dissipated in the cavity is made equal to the energy given by the atoms. Equations (19) and (20) and the definition of  $b$  lead to the fundamental relation

$$b = 2k |\delta_{\mu\mu'}|. \quad (23)$$

The ambiguity on the sign of  $b$ , resulting from this power self-consistent approach, has been removed by making the field consistent with its definition through Eqs. (3) and (14).

### 3. Maser master equations

For simplicity of presentation, we will divide the following analysis in two parts for two conditions realized in practice. Using the adiabatic approximation where the optical coherences are assumed to evolve much faster than the ground-state coherence, and using the results derived above, the system of equations (6)–(11) can be reduced to a system of two equations describing entirely the phenomenon of stimulated emission in a self consistent approach. In the following paragraphs we will discuss only this reduced set of equations.

(a) In the first part we assume that the optical radiation fields are exactly tuned to the optical transitions, that is  $\Delta_0 = 0$ . In that case the rate equations are reduced to

$$\dot{\Delta} + [\gamma_1 + (1 + \beta^2)\Gamma_p]\Delta = -4k |\delta_{\mu\mu'}|^2 + (1 - \beta^2)\Gamma_p, \quad (24)$$

$$\delta_{\mu\mu'} + [\gamma_2 + (1 + \beta^2)\Gamma_p - k\Delta + i(\Omega_\mu - k\psi\Delta)]\delta_{\mu\mu'} = -\beta\Gamma_p,$$

where  $\beta$  is the ratio of the two optical Rabi frequencies,  $(\omega_{R2}/\omega_{R1})$ ,  $\Gamma_p = \omega_{R1}^2/2\Gamma^*$ , and  $\psi$  stands for

$$\psi = 2Q_L \frac{\Delta\omega_c}{\omega_{12}}, \quad (25)$$

which has been assumed to be  $\ll 1$ .

(b) In the second case we assume that the cavity is exactly tuned, that is,  $\Delta\omega_c = 0$  and the two optical Rabi frequencies have the same intensity. We obtain

$$\dot{\Delta} + [\gamma_1 + 2\Gamma_p/(1 + \delta_0^2)]\Delta = -4k |\delta_{\mu\mu'}|^2 + 4\Gamma_p \delta_{\mu\mu}^i \delta_0 / (1 + \delta_0^2), \quad (26)$$

$$\delta_{\mu\mu'} + [\gamma_2 - k\Delta + 2\Gamma_p/(1 + \delta_0^2) + i\Omega_\mu]\delta_{\mu\mu'} = -\Gamma_p/(1 + \delta_0^2) - i\Gamma_p\Delta\delta_0/(1 + \delta_0^2),$$

where  $\delta_0$  stands for  $\Delta_0/(\Gamma^*/2)$ .

These two systems (24) and (26) describe, in a self-consistent approach, most of the behaviors of the atomic ensemble of alkali atoms placed inside a microwave cavity. It is also possible to write a system for  $\Delta$  and  $\delta$  that takes into account all the possible parameter variations, but it becomes way less transparent to analytical interpretation.

### C. Stimulated emission and the difference between CPT and IOP masers

The above set of equations will now be applied to various cases encountered in experimental situations.

#### 1. Dynamical solutions

The situation where  $\beta = 1$  represents the case of the ideal CPT maser. The coherent pumping rates from each hyperfine ground-state level are equal. In that case, assuming the cavity to be tuned and the laser frequency difference to be equal to the hyperfine frequency, the system (24) become

$$\text{CPT maser} \Rightarrow \begin{cases} \dot{\Delta} + (\gamma_1 + 2\Gamma_p)\Delta = -4k(\delta'_{\mu\mu'})^2, \\ \delta'_{\mu\mu'} + (\gamma_2 + 2\Gamma_p)\delta'_{\mu\mu'} = k\Delta\delta'_{\mu\mu'} - \Gamma_p. \end{cases} \quad (27)$$

It is noted that under the condition of exact tuning of the laser and of the cavity, the term  $\delta_{\mu\mu'}$  is real. It is interesting to point out that the pumping rate  $\Gamma_p$  acts as a transverse pumping rate creating a ground-state hyperfine coherence in the ensemble without affecting the populations of the ground-state levels. The analytical solution of the system (27) is not known when  $\Gamma_p \neq 0$ . The response of the system to a laser pulse (dynamical behavior) is analyzed by numerical integration. The results are shown in Fig. 3 for a particular set of physical parameters. Radiation damping is present in the transient response of the system because of the relatively high gain parameter chosen,  $k = 3000 \text{ s}^{-1}$ . An oscillation in the switching-on transient and a reduced decay time in the switching-off transient are observed. For the same reason, the effect of the microwave field is readily observed on

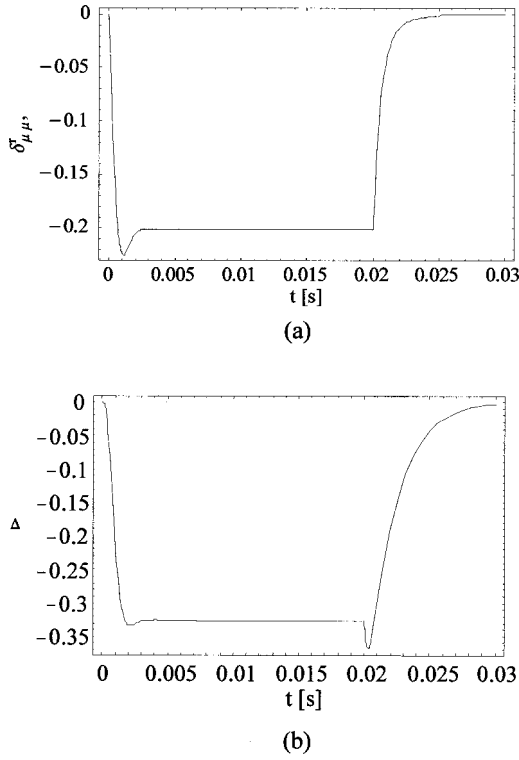


FIG. 3. Calculated dynamic response of the hyperfine ground-state coherence (a) and population difference (b) to a laser pulse width. The parameters are:  $\gamma_2 = 500 \text{ s}^{-1}$ ;  $k = 3000 \text{ s}^{-1}$ ;  $\Gamma_p = 500 \text{ s}^{-1}$ . The laser pulse length is 20 ms.

the relative populations of the two ground-state hyperfine levels. The population difference becomes negative upon the rise of the coherence, which creates the microwave field in the cavity. In the absence of a cavity, no microwave field would be present, and the population would remain equal ( $\Delta = 0$ ) even for large values of  $\delta_{\mu\mu'}$ .

In the situation where  $\beta = 0$  ( $\omega_{R2} = 0$ ,  $\omega_{R1} = \omega_R$ ), optical transitions are excited only from the lower ground-state hyperfine level and a population inversion is created. This situation corresponds to the case of the IOP maser using a laser as the source of pumping. System (24) for  $\Delta\omega_c$  and  $\Omega_\mu$  both equal to zero, leads to

$$\text{IOP maser} \Rightarrow \begin{cases} \dot{\Delta} + (\gamma_1 + \Gamma_p)\Delta = -4k(\delta_{\mu\mu'}^r)^2 + \Gamma_p, \\ \dot{\delta}_{\mu\mu'}^r + (\gamma_2 + \Gamma_p)\delta_{\mu\mu'}^r = k\Delta\delta_{\mu\mu'}^r. \end{cases} \quad (28)$$

In the present case, no coherence is created at the ground-state hyperfine frequency by the laser that acts essentially as a longitudinal pumping source. The above system of equations has a trivial solution with the coherence  $\delta_{\mu\mu'} = 0$  at all

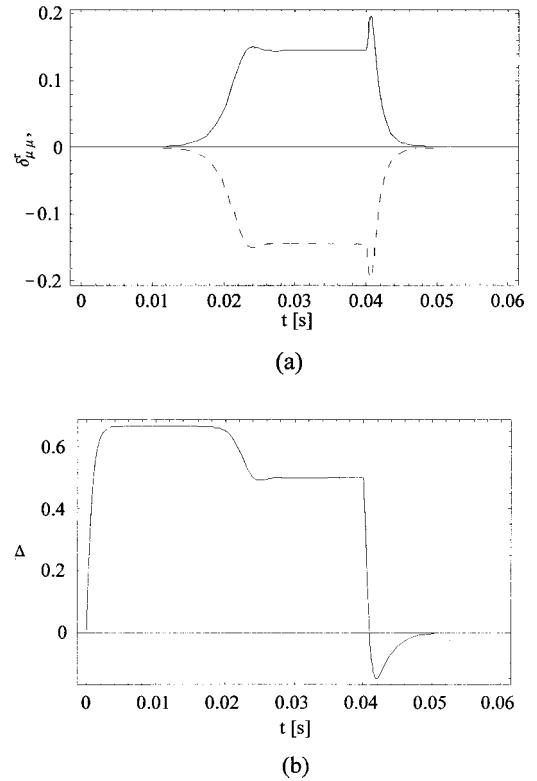


FIG. 4. Theoretical dynamical behavior of the intensity-pumped maser over threshold. (a) ground-state coherence, (b) population difference. The parameters are:  $k = 3000 \text{ s}^{-1}$ ,  $\gamma_2 = 500 \text{ s}^{-1}$ , and  $\Gamma_p = 1000 \text{ s}^{-1}$ . The laser pulse width is 40 ms.

times. The population difference then remains equal to  $\Gamma_p / (\gamma_1 + \Gamma_p)$ . However, with an initial condition such as  $\delta_{\mu\mu'} \neq 0$ , it is possible to find, by numerical integration, non-trivial solutions of the system (28). A threshold condition exists for the creation of the coherence  $\delta_{\mu\mu'}$ . The results for a particular choice of parameters are shown in Fig. 4 for the response of the system to a laser pulse as in the previous case. A delay in the buildup of coherence in the system is readily observed and depends on the amplitude of initial conditions set for  $\delta_{\mu\mu'}$ . The population difference  $\Delta$ , however, builds up at a rate proportional to the pumping rate  $\Gamma_p$  from the beginning of the light pulse. Similar effects as those seen above in the CPT maser in connection to radiation damping and reported in Ref. [20], are observed in the present case.

## 2. Steady-state solution

Steady-state solutions for the above systems are readily obtained by setting all time derivatives equal to zero. In the case of the CPT maser, assuming for simplicity  $\gamma_1 = \gamma_2$  the following set of equations are obtained:

$$\text{CPT maser} \Rightarrow \begin{cases} \Delta_e = -\frac{4k}{\gamma_2 + 2\Gamma_p}(\delta_{\mu\mu'}^r)_e^2, \\ (\delta_{\mu\mu'}^r)_e^3 + \frac{(\gamma_2 + 2\Gamma_p)^2}{4k^2}(\delta_{\mu\mu'}^r)_e + \frac{\Gamma_p(\gamma_2 + 2\Gamma_p)}{4k^2} = 0, \end{cases} \quad (29)$$

where the subscript  $e$  stands for equilibrium. In the present case,  $\delta_{\mu\mu'}^i = 0$  at all times because  $\Omega_\mu = 0$ , and the cavity and the lasers are assumed to be tuned exactly to their respective resonance. The above system has always only one real solution with  $\Delta_e \leq 0$  and  $(\delta_{\mu\mu'}^r)_e \leq 0$ , which represents a stationary point of operation of the atomic ensemble coupled to the microwave cavity. The stability of this equilibrium point may be easily analyzed through the eigenvalues of the Jacobian associated with system (27): it turns out to be a stable spiral when

$$k^2(\delta_{\mu\mu'}^r)_e^2 < 2(\gamma_2 + 2\Gamma_p)^2 \quad (30)$$

or a stable node in the opposite case. The main physical properties of the stationary solution provided by Eq. (29) are (i) no threshold exists for the coherent emission; (ii)  $\rho_{\mu\mu} > \rho_{\mu'\mu'}$ : the population of the lower level is always larger than the population of the higher level. In the case of the IOP maser, the nature of the pumping introduces a fundamental change in the behavior of the atomic ensemble. At equilibrium the system admits three equilibrium points depending on the initial conditions. Assuming for simplicity that  $\gamma_1 = \gamma_2 = \gamma$  one obtains:

$$\begin{aligned} \text{IOP maser} \Rightarrow P_1 & \begin{cases} \Delta_e = \Gamma_p / (\gamma + \Gamma_p) \\ (\delta_{\mu\mu'}^r)_e = 0 \end{cases}, \\ P_2, P_3 & \begin{cases} \Delta_e = (\gamma + \Gamma_p) / k, \\ (\delta_{\mu\mu'}^r)_e = \pm \frac{1}{2} \sqrt{\frac{\Gamma_p}{k} - \left(\frac{\gamma + \Gamma_p}{k}\right)^2}. \end{cases} \end{aligned} \quad (31)$$

The existence of point  $P_1$  is always possible and represents an atomic system with inverted population in the ground state but with no emitted radiation; it is a stable point when  $k < (\gamma + \Gamma_p)^2 / \Gamma_p$ , otherwise it is a saddle point. The second and third points  $P_2$  and  $P_3$  exist only when  $k > (\gamma + \Gamma_p)^2 / \Gamma_p$ , since  $(\delta_{\mu\mu'}^r)_e$  must be real. The choice between the two solutions ( $\pm$  sign) is defined by the initial conditions. The condition just mentioned is required for free oscillation of the system. Moreover, for  $k > 4\gamma$ , there is only a well-defined range of values of  $\Gamma_p$  that allows the self-sustainment of the maser oscillation. This last condition is related to the oscillation condition derived in Refs. [14] and [21] for ensembles of Rb and Cs alkali-metal atoms. In those cases, a different mathematical context was used taking into account a more complex ground-state manifold than the one considered in the present calculation. From the physical point of view we have in this case the following situation: (i) a threshold exists for a stable coherent microwave emission. This threshold requires  $k > 4\gamma$ ; (ii)  $\rho_{\mu'\mu'} > \rho_{\mu\mu}$ : the ground-state populations are inverted; (iii) above threshold there is a well-defined range of pumping rates where maser emission can be self-sustained. As mentioned previously in the dynamic solution, the system does not get into oscillation and reach the equilibrium points  $P_2$  or  $P_3$  without an external excitation such as that provided in practice by noise.

The fundamental difference between the CPT and the IOP masers is made more evident in Fig. 5, which shows the

operating behavior of the two oscillators in the  $\Delta$ - $\delta$  plane: in the pumped maser no emission takes place until the population inversion  $\Delta$  has reached a significant value, while in the CPT case coherent emission is present at times  $t = 0^+$  where  $\Delta \sim 0$ .

The behavior of the two types of masers is shown in Fig. 6, in which the emitted power, proportional to  $k(2\delta_{\mu\mu'}^r)_e^2$ , is plotted as a function of the pumping rate for the two cases considered in this section. Table I summarizes the main differences between the CPT and the IOP masers. Even if both masers emit coherent radiation, the CPT maser has mostly the features of a passive maser.

#### D. The mixed or intermediate case ( $0 < \beta < 1$ or $\beta > 1$ )

So far we have considered the two extreme cases of  $\beta = 1$ , corresponding to the pure CPT situation, and  $\beta = 0$ , describing the pure IOP maser in the framework of a three-level model. We now wish to examine the cases  $0 < \beta < 1$  and  $\beta > 1$ , which represent an intermediate excitation scheme where both CPT and IOP are present. Assuming again the conditions where  $\Delta_0 = 0$ ,  $\Delta\omega_c = 0$ , and  $\Omega_\mu = 0$ , Eqs. (24) may be written as

$$\begin{aligned} \Delta + [\gamma_1 + (1 + \beta^2)\Gamma_p]\Delta &= -4k(\delta_{\mu\mu'}^r)^2 + (1 - \beta^2)\Gamma_p, \\ \delta_{\mu\mu'}^r + [\gamma_2 + (1 + \beta^2)\Gamma_p]\delta_{\mu\mu'}^r &= k\Delta\delta_{\mu\mu'}^r - \beta\Gamma_p. \end{aligned} \quad (32)$$

It is clear from these equations that the atomic ensemble is now submitted to both a longitudinal pumping rate  $(1 - \beta^2)\Gamma_p$  and a transversal pumping rate  $\beta\Gamma_p$ . An analysis of the equilibrium points of Eqs. (32) shows that when  $\beta \geq 1$  only one equilibrium point exists. When  $0 \leq \beta < 1$  one or three equilibrium points exist depending on the system gain. The stability of the equilibrium points may be again analyzed through the eigenvalues of the Jacobian associated to the system of equations.

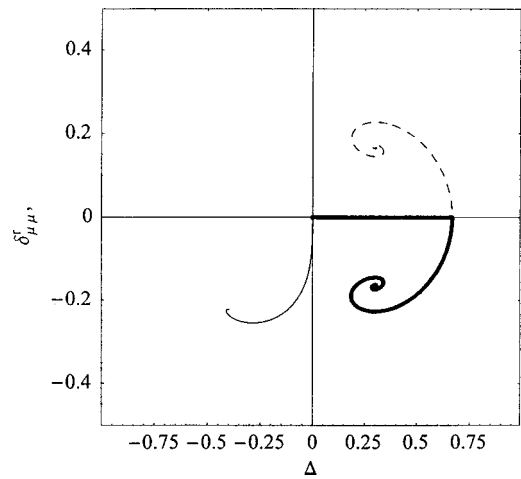


FIG. 5. Parametric plot of the coherence versus population inversion for the CPT (—) maser and for intensity-pumped (---) maser. In the second case a symmetric solution (---) is also possible (depending on the initial value of  $\delta_{\mu\mu'}^r$ ). The parameters are:  $k = 5000 \text{ s}^{-1}$ ,  $\gamma_2 = 500 \text{ s}^{-1}$ , and  $\Gamma_p = 1000 \text{ s}^{-1}$ .

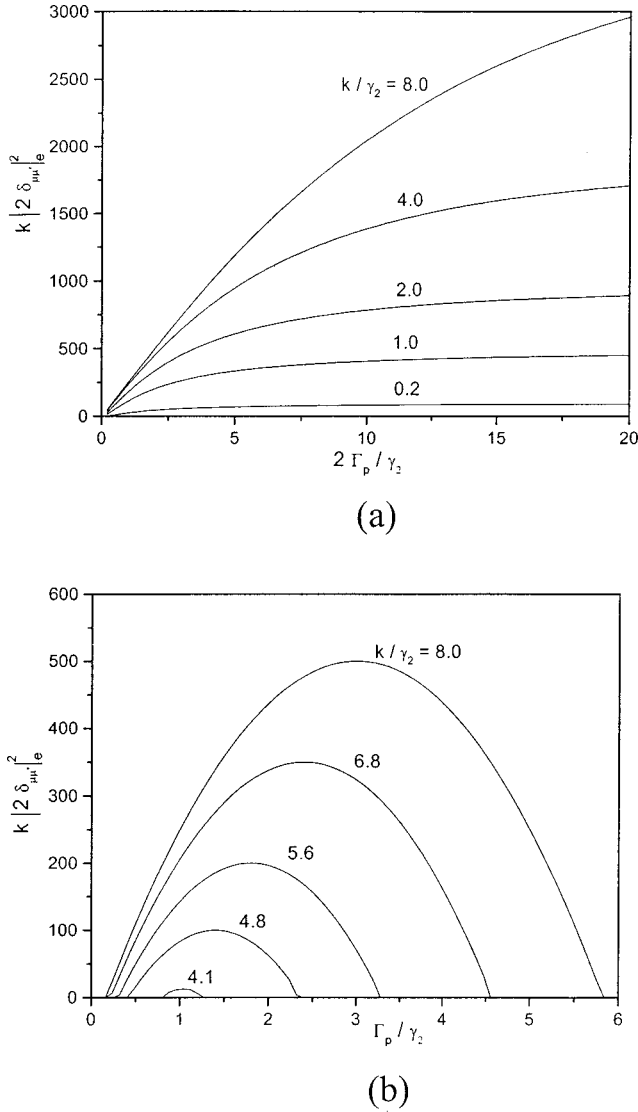


FIG. 6. Calculated emitted power for (a) the CPT maser, (b) the IOP maser vs the pumping rate; in this case the curves are parabolas of the equation  $k(2\delta_{\mu\mu'}^e)^2 = \Gamma_p - (\gamma_2 + \Gamma_p)^2/k$ . Coherence relaxation rate  $\gamma_2$  is  $500 \text{ s}^{-1}$ .

A parametric representation, in the  $\Delta$ - $\delta$  plane, of the dynamical behavior of the system, is shown in Fig. 7, where the endpoints of the stable spirals describe the equilibrium reached by the atomic ensemble for different values of  $\beta$ . In this figure, going from (a) to (d) the system moves from an IOP to a CPT configuration. The various spirals in each of the figures correspond to different initial conditions at  $t=0$  ( $-0.8 < \Delta < 0.8$  and  $-0.4 < \delta_{\mu\mu'}^r < 0.4$ ).

The ‘locus’ of the equilibrium points spanned by the system in the  $\Delta$ - $\delta$  plane when the  $\beta$  parameter is adiabati-

cally changed from  $\beta=0$  to  $\beta=1$ , is reported in Fig. 8. Increasing the value of  $\beta$  in the upper branch (starting point  $\beta=0$ , pure intensity pumping), a critical value is reached ( $\beta \sim 0.1$ ) for the set of parameters chosen in Fig. 7, where the system undergoes a sudden transition to the lower branch. On the contrary, changing adiabatically the value of  $\beta$  in the lower branch, the system never jumps to the upper one: the lower branch represents a stable state of the atomic system, while the upper branch behaves as a metastable state. When the feedback of the cavity is reduced, lowering the value of  $k$  below  $4\gamma_2$ , only the lower stable branch remains.

### III. LINE SHAPES AND FREQUENCY SHIFTS

In view of applications of the CPT microwave coherent emission to the field of atomic frequency standards, it is important to examine the emission profile of the CPT maser in relation to line shape and frequency of its maximum. In the following discussion, we consider only the physical effects related to the time-dependent perturbation Hamiltonian: these include the shift caused by the microwave cavity tuning (cavity pulling), the light shift, and the microwave power shift. The frequency shifts, which can be taken into account in the unperturbed Hamiltonian as time-independent perturbations due to the Zeeman effect, or collisions of alkali atoms with the buffer gas, are not considered here. We will not consider either the light shift caused by off-resonance light such as sidebands in the laser spectrum (power and quadratic). These effects have been discussed in Refs. [4] and [22].

#### A. Low feedback

We first examine the case of the emission profile for  $k \ll \gamma_2$  (low  $Q$  cavity and/or low number of atoms). From Eq. (23) this condition implies  $b \cong 0$ . In this case, the system of equations (6)–(11) is linear and has been examined in Ref. [4]. We recall here some useful results for a better understanding of the effects related to the reaction of the atomic ensemble to the presence of the cavity, effects which will be derived later in this section. Solving the system of Eqs. (6)–(11) for  $\Delta_0=0$ ,  $\omega_{R1}=\omega_{R2}=\omega_R$ , and  $\Delta\omega_c=0$  one obtains for the stationary case:

$$|\delta_{\mu\mu'}|^2 = \frac{\Gamma_p^2}{(\gamma_2 + 2\Gamma_p)^2 + \Omega_\mu^2}. \quad (33)$$

Equation (33), taking into account Eq. (20), describes the emission profile of the system uncoupled from the microwave cavity. In that case, the line shape is a Lorentzian centered at  $\Omega_\mu=0$  (that is, at the hyperfine frequency) and with a full width at half-maximum (FWHM)  $\Delta\omega_{1/2}=2(\gamma_2$

TABLE I. Main physical differences between the CPT and the IOP masers studied in the text.

Maser type	$\Delta = \rho_{\mu'\mu'} - \rho_{\mu\mu}$	Threshold	$\omega_{\text{out}}$	$P_{\text{out}}$
CPT	$< 0$	no	$\omega_1 - \omega_2$	Saturation vs pumping
IOP	$> 0$	$k/\gamma_2 = 4$	$\omega_{\mu'\mu}$	Maximum vs pumping

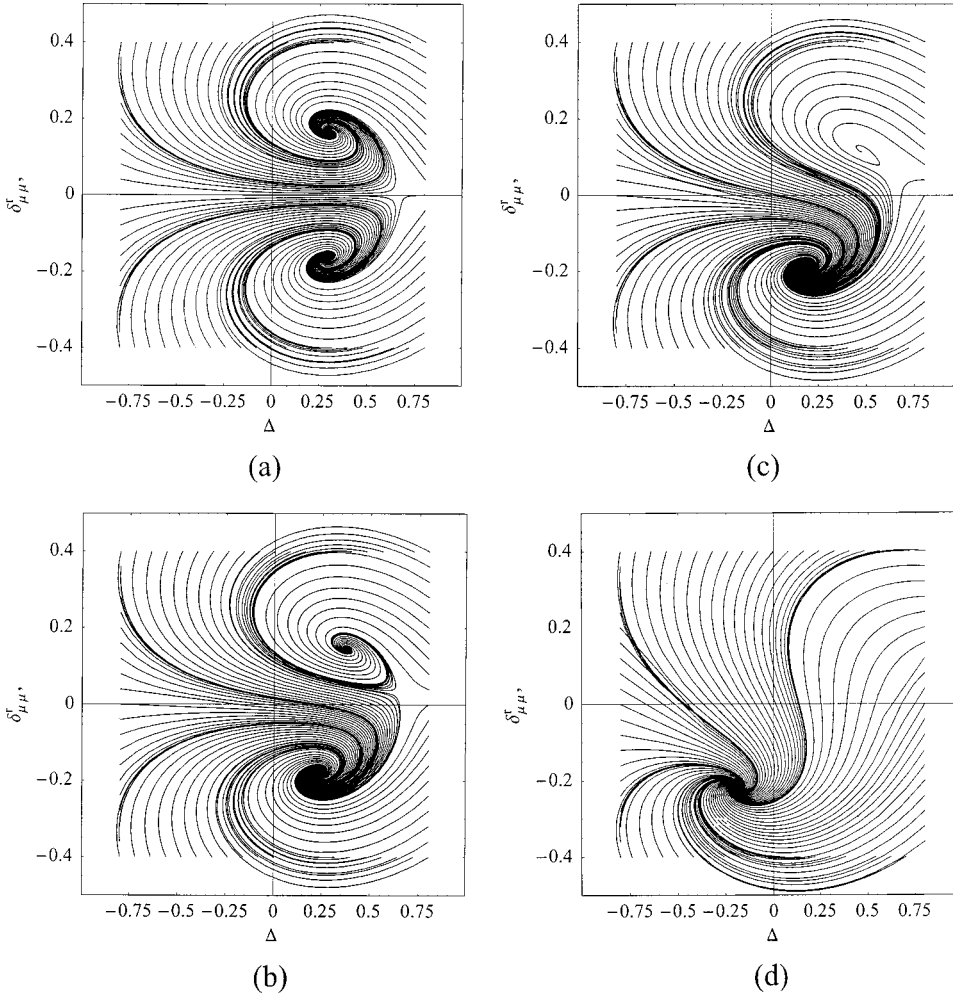


FIG. 7. Theoretical dynamical behavior of the atomic ensemble for the case  $0 < \beta < 1$  (mixed or intermediate case). The parameters chosen are:  $\gamma_2 = 500 \text{ s}^{-1}$ ;  $k = 5000 \text{ s}^{-1}$ ;  $\Gamma_p = 1000 \text{ s}^{-1}$ . (a)  $\beta^2 = 3 \times 10^{-6}$ , (b)  $\beta^2 = 3 \times 10^{-3}$ , (c)  $\beta^2 = 1 \times 10^{-2}$ , and (d)  $\beta^2 = 0.4$ . Each trace corresponds to different initial conditions for  $\Delta$  and  $\delta_{\mu\mu}^r$ , as explained in the text. The system evolves from an IOP maser ( $\beta$  very small  $\sim 0$ ) in ‘‘a’’ to a CPT maser ( $\beta$  approaches 1) in ‘‘d.’’ The center of the spirals correspond to the equilibrium solution of Eqs. (32).

$+2\Gamma_p$ ). The cavity pulling shift of the emission profile can be calculated from Eqs. (20) and (33) and is given by

$$\Delta\omega = -\left(\frac{Q_L}{Q_a}\right)^2 \Delta\omega_c, \quad (34)$$

where  $Q_a$  is the atomic resonance quality factor defined as  $Q_a = \omega_{\mu'\mu} / \Delta\omega_{1/2}$ . In the more general case, when  $\Delta_0 \neq 0$  and  $\omega_{R1} \neq \omega_{R2}$ , a shift of the emission profile is found solving the system of Eqs. (6)–(11) in the stationary limit and with  $\beta \sim 1$ , one obtains

$$\Delta\omega_{LS} = -\frac{(1-\beta^2)\omega_{R1}^2}{4} \left\{ \frac{\Delta_0}{(\Gamma^*/2)^2 + \Delta_0^2} \right\}. \quad (35)$$

In the usual experimental conditions,  $\Delta_0 \ll \Gamma^*/2$ , and this shift is also called ‘‘linear light shift.’’ The emission profile is always a Lorentzian but its maximum is shifted by the amount given by Eq. (35). In this case it may also be shown that the population difference  $\Delta$  in the ground state is given by

$$\Delta = \frac{\Gamma_p(1-\beta^2)}{\gamma_1 + \Gamma_p(1+\beta^2)}. \quad (36)$$

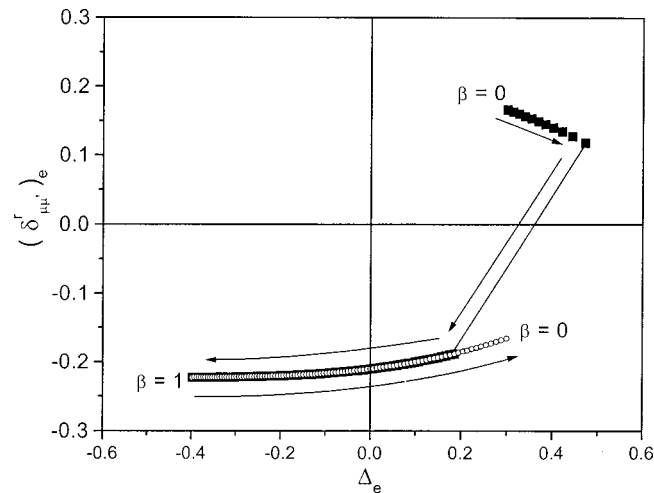


FIG. 8. Locus of the equilibrium solutions for the CPT and IOP masers for the parameters chosen in the dynamic response represented in Fig. 7.

A partial intensity optical pumping is present in this case due to the imbalance of the optical radiation fields, which is responsible for the linear light shift reported above.

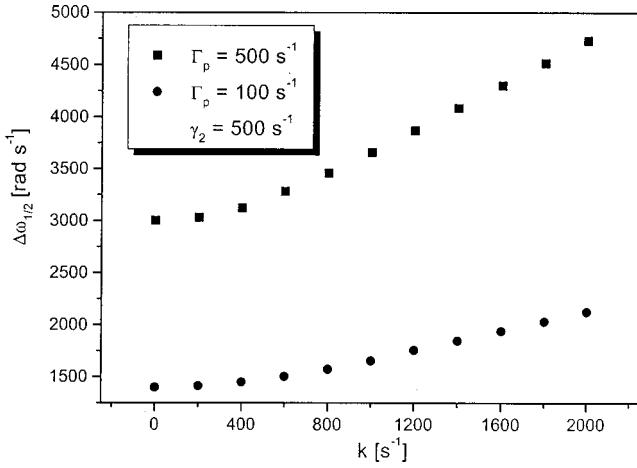


FIG. 9. Calculated CPT maser emission profile linewidth (FWHM) as a function of the gain parameter  $k$  for two cases of the pumping rate and for  $\omega_{R1} = \omega_{R2}$ ,  $\Delta_0 = 0$ , and  $\Delta\omega_c = 0$ .

### B. High feedback

When the microwave Rabi frequency is not negligible relative to the relaxation and pumping rates, the following effects are present:

- (i) **microwave broadening**: the microwave field of the cavity strongly couples the hyperfine levels of the ground state producing a broadening of the emission profile, a phenomenon commonly called power broadening [15];
- (ii) **cavity pulling**: the dephasing with respect to quadrature of the generated microwave field versus the oscillating magnetization, as given by Eq. (14) when  $\Delta\omega_c \neq 0$ , introduces an additional shift of the emission profile;
- (iii) **microwave shift**: the imbalance of the ground-state populations ( $\Delta \neq 0$ , as seen, for example, in Fig. 5), produced by the microwave field stored in the cavity even when  $\omega_{R1} = \omega_{R2}$ , introduces a residual optical pumping that shifts the emission profile when  $\Delta_0 \neq 0$  as in the case of the linear light shift.

The first two effects may be made evident from a direct analysis of system (24), setting  $\beta = 1$ :

$$\dot{\Delta} + (\gamma_1 + 2\Gamma_p)\Delta = -4k|\delta_{\mu\mu'}|^2, \quad (37)$$

$$\dot{\delta}_{\mu\mu'} + [\gamma_2 + 2\Gamma_p - k\Delta + i(\Omega_\mu - k\psi\Delta)]\delta_{\mu\mu'} = -\Gamma_p.$$

From the second equation of system (37) in the stationary limit ( $\partial/\partial t \rightarrow 0$ ) we have

- (i) a **microwave broadening** equal to  $-k\Delta$ . It is readily shown that

$$-k\Delta = b^2/(\gamma_1 + 2\Gamma_p), \quad (38)$$

which is essentially the saturation factor that is encountered in magnetic resonance and that causes power broadening.

- (ii) a **cavity pulling** equal to  $k\psi\Delta$ . Using the results derived previously and Eq. (25) in the case of small cavity detuning, we obtain

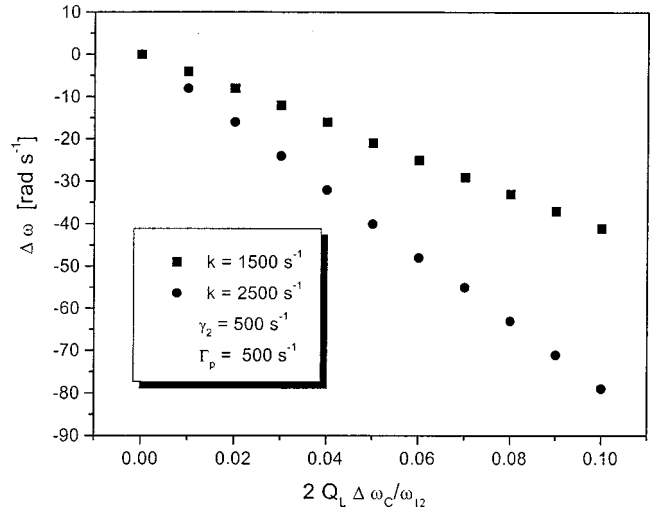


FIG. 10. Calculated frequency shift of the emission profile versus  $2Q_L\Delta\omega_c/\omega_{12}$  (cavity tuning) and for the case  $\omega_{R1} = \omega_{R2}$ ,  $\Delta_0 = 0$ .

$$k\psi\Delta = \frac{Q_L}{Q_a}\Delta\omega_c(S-1), \quad (39)$$

where  $S$  is the ratio of the total power broadened linewidth including all broadening mechanisms,  $\Delta\nu'_{1/2}$ , to the linewidth caused only by relaxation and optical pumping  $\Delta\nu^n_{1/2}$ :

$$S = \frac{\Delta\nu'_{1/2}}{\Delta\nu^n_{1/2}} = \frac{4k^2|\delta_{\mu\mu'}|^2}{(\gamma + 2\Gamma_p)^2} + 1. \quad (40)$$

A similar analysis may be done also for the microwave shift. In that case system (26) is used. The last term in the second equation, the imaginary term, is responsible for the microwave shift introducing a coupling to the population difference  $\Delta$ .

The results of a numerical integration of the various equations used in the present discussion are shown in Figs. 9, 10, and 11. The broadening of the emission profile given by Eq. (38) is reported in Fig. 9 for two values of the pumping rate. The shape of the profile, Lorentzian for  $k \rightarrow 0$ , is not significantly modified in the range of  $k$  considered in the figure. The shift of the emission profile maximum with cavity tuning for two values of the gain factor  $k$  is shown in Fig. 10 for the case  $\beta = 1$  and  $\Delta_0 = 0$ . Finally the shift of the emission profile maximum as a function of the laser tuning  $\Delta_0$ , for  $\beta = 1$  and  $\Delta\omega_c = 0$ , for three values of the gain  $k$ , is shown in Fig. 11. This shift is similar to the linear light shift mentioned above, but in the present case it is due to the optical detuning acting through the microwave power, which reacts on the ensemble and alters both the coherence and the populations of the ground-state hyperfine levels.

## IV. CONCLUSIONS

In this paper we have developed a fully self-consistent theory of the CPT maser, taking into account the feedback of the microwave cavity field on the atomic ensemble. The cavity feedback destroys partially the intrinsic symmetry of the

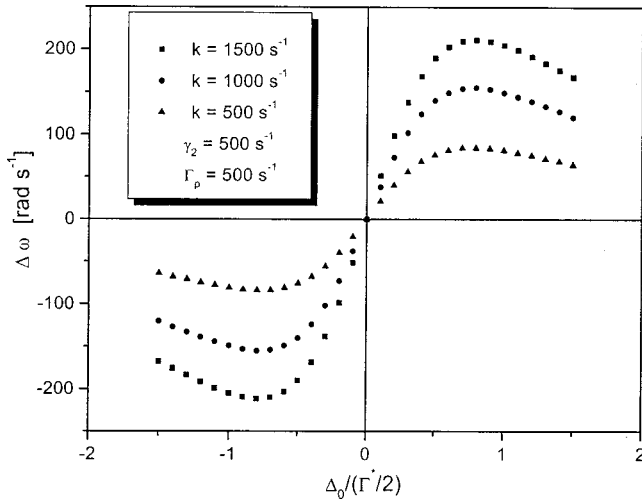


FIG. 11. Calculated microwave shift (power shift) of the CPT maser emission profile for three values of the gain parameter  $k$  and for  $\omega_{R1} = \omega_{R2}$ ,  $\Delta\omega_c = 0$ .

$\Lambda$  excitation scheme, resulting in an extra broadening of the emission profile, which we have identified as microwave broadening. The cavity feedback creates also radiation damping, which is visible under transient operation. We have also investigated the effect of the cavity feedback on the frequency of the maximum of emission to the CPT maser. It has been shown theoretically that the cavity pulling effect is enhanced by the cavity feedback to become linear with the ratio of the cavity  $Q$  to the atomic line  $Q$ , ( $Q_L/Q_a$ ) as in the active IOP maser at high value of the gain factor  $k$ . An additional shift of the emission profile related to the microwave Rabi frequency is present when  $\Delta_0 \neq 0$ .

The theoretical calculations were also extended to the case of intensity optical pumping by a simple alteration of the relative intensities of the two excitation radiation fields used in the CPT approach. It was shown that the IOP maser and the CPT maser are natural extensions of each other, but

that their physical behavior are basically different. The IOP maser is characterized mainly by the presence of an oscillation threshold in relation to cavity  $Q$ , atomic density and pumping rate creating the population inversion. On the other hand, the CPT maser is characterized by the absence of a threshold regarding the parameters just mentioned, as well as the absence of population inversion in the ground state. Furthermore, in the IOP maser, emission takes place essentially at the hyperfine frequency although shifted by various perturbations, while in the CPT maser, coherent emission takes place at a frequency corresponding to the difference between the frequency of the laser radiation fields used in the  $\Lambda$  scheme. This last behavior is characteristic of passive masers although we have shown that the CPT maser, in high-gain situations, behaves in a way very similar to an active maser in relation to several effects such as radiation damping, cavity frequency pulling, and power broadening.

The present calculations are in agreement with results already published on the IOP Rb maser [14]. In the case of the CPT maser some preliminary results have been obtained on the radiation damping effect. A comparison of the theoretical conclusions here reported with the experimental results is in progress and will be made the object of a future report.

For what concerns the practical realization of an atomic frequency standard, it is worth noting that the CPT maser allows a better control of the light shift effect and, because there is no threshold, a reduction of the cavity pulling effect. The short term stability of the CPT maser is expected to be a little worse than the IOP maser, also because the CPT maser is dominated by white frequency noise ( $\tau^{-1/2}$ ) instead of white phase noise ( $\tau^{-1}$ ), but the long term stability and drift are on the contrary expected to be significantly lower.

#### ACKNOWLEDGMENTS

The authors wish to thank N. Beverini, E. Maccioni, and G. Modugno for their help. This work has been partially supported by ASI (Italian Space Agency).

- 
- [1] A. Godone, F. Levi, and J. Vanier, Phys. Rev. A **59**, R12 (1999).
  - [2] F. Levi, A. Godone, and J. Vanier, IEEE Trans. Ultrason. Ferroelectr. Freq. Control **46**, 609 (1999).
  - [3] J. Vanier, A. Godone, and F. Levi, *Conference on Precision Electromagnetic Measurements, Washington, D.C., 1998* (T. L. Nelsen, Washington, DC, 1998); A. Godone, F. Levi, and J. Vanier, IEEE Trans. Instrum. Meas. **48**, 504 (1999).
  - [4] J. Vanier, A. Godone, and F. Levi, Phys. Rev. A **58**, 2345 (1998).
  - [5] G. Alzetta, A. Gozzini, L. Moi, and G. Orriols, Nuovo Cimento B **36B**, 5 (1976).
  - [6] A. Aspect, E. Arimondo, R. Kaiser, N. Vansteenkiste, and C. Cohen-Tannoudji, J. Opt. Soc. Am. B **11**, 2112 (1989).
  - [7] M. O. Scully, Phys. Rep. **219**, 191 (1992).
  - [8] H. Lee, M. Fleischauer, and M. O. Scully, Phys. Rev. A **58**, 2587 (1998).
  - [9] N. Cyr, M. Têtu, and M. Breton, IEEE Trans. Instrum. Meas. **42**, 640 (1993).
  - [10] F. Levi, A. Godone, C. Novero, and J. Vanier, *Proceedings of the 11th European Frequency and Time Forum, Neuchâtel, Switzerland, 1997* (FSRM, Neuchâtel, 1997).
  - [11] A. S. Zibrov, H. G. Robinson, V. L. Velichansky, V. V. Vasiliev, L. Holdberg, E. Arimondo, M. D. Lukin, and M. O. Scully, in *Proceedings of the 5th Symposium on Frequency Standards and Metrology*, edited by J. C. Bergquist (World Scientific, Singapore, 1995), p. 490.
  - [12] D. Kleppner, H. M. Goldenberg, and N. F. Ramsey, Phys. Rev. **126**, 603 (1962).
  - [13] P. Davidovits, Appl. Phys. Lett. **5**, 15 (1964).
  - [14] J. Vanier, Phys. Rev. **168**, 129 (1968).
  - [15] J. Vanier and C. Audoin, *The Quantum Physics of Atomic Frequency Standards* (Adam Hilger, Bristol, 1989).
  - [16] R. H. Dicke, Phys. Rev. **89**, 472 (1953).

- [17] F. Levi, A. Godone, J. Vanier, S. Micalizio, and G. Modugno, Europhys. J. D (to be published).
- [18] G. Orriols, Nuovo Cimento B **53B**, 1 (1979).
- [19] R. E. Collin, *Field Theory of Guided Waves*, 2nd ed. (IEEE, New York, 1991).
- [20] J. Vanier, Phys. Rev. Lett. **18**, 33 (1967).
- [21] J. Vanier and F. Strumia, Can. J. Phys. **54**, 2355 (1976).
- [22] F. Levi, A. Godone, and J. Vanier, IEEE Trans. Ultrason. Ferroelectr. Freq. Control **47**, 466 (2000).